Metal–Ammonia Solutions

International Edition: DOI: 10.1002/anie.201604282
German Edition: DOI: 10.1002/ange.201604282

Metal Transition in Sodium–Ammonia Nanodroplets

*Sebastian Hartweg, Adam H. C. West, Bruce L. Yoder, and Ruth Signorell**

Abstract: *The famous nonmetal-to-metal transition in Na–ammonia solutions is investigated in nanoscale solution droplets by photoelectron spectroscopy. In agreement with the bulk solutions, a strong indication for a transition to the metallic state is found at an average metal concentration of 8.8 ± 2.2 mole%. The smallest entity for the phase transition to be observed consists of approximately 100–200 solvent molecules. The quantification of this critical entity size is a stepping stone toward a deeper understanding of these quantum–classical solutions through direct modeling at the molecular level.*

We report the characterization of sodium–ammonia nanodroplets for average metal concentrations between 1.2 and 8.8 mole%-metal (MPM) using angle-resolved photoelectron imaging. The concentration-dependent properties of metal-ammonia solutions have intrigued chemists ever since the observation of their fascinating, concentration-dependent colors by Sir Humphry Davy and W. Weyl more than 150 years ago.[1] A large amount of experimental and theoretical work followed these pioneering studies (see the review by Zurek, Edwards, and Hoffmann[2] and references therein). For increasing metal concentrations, the following picture emerged from these investigations (see, for example, Figure 2 and Figure 3 in Ref. [2] for lithium): Dilute bulk solutions behave like electrolytes, consisting of isolated solvated metal ions and electrons (solvated electrons localized in Å-sized cavities[2,3]) at very low concentrations ($\lesssim 10^{-3}$ MPM) and of associated solvated cations and electrons (ion pairs) at concentrations between approximately 10^{-3}–10^{-2} MPM. In the intermediate concentration regime up to approximately 1 MPM, magnetic measurements provide evidence that electron spin-pairing takes place. The transition to the metallic state (TMS), in which the conductivity increases with increasing concentration, occurs at concentrations of approximately 1–10 MPM. The nonmetal–metal transition is the origin of the famous color change from the deep blue of the nonmetallic bulk liquid to the copper-gold of the metallic bulk liquid. The TMS in sodium–ammonia solutions is accompanied by liquid–liquid phase separations below the upper consolute temperature of 231.5 K (Figure 10 in Ref. [4]). This miscibility gap results in the broad MPM range that is usually indicated for the TMS. Na–ammonia solutions solidify between about 160 and 190 K.[4,5]

Various methods were used to characterize the TMS, including, visual inspection[6] and resistance,[7] conductance,[5a,b] Hall-effect[8] and neutron diffraction measurements,[9] as well as theoretical studies.[3d,4] However, concentration-dependent photoelectron spectra (PES) that provide direct information on the electron binding energy (eBE) have not been reported for bulk solutions, likely owing to the inherent difficulties with liquid-bulk phase PES. The only photoemission data reported are energy-dependent electron yield measurements that provide photoelectric threshold (PET) values.[10] The bulk PET increases from 1.42 eV for dilute nonmetallic Na–ammonia solutions with 0.83 MPM to a value between 1.5 and 1.6 eV for concentrated metallic solutions of 10–16 MPM. The phase change from nonmetallic to metallic solutions is also accompanied by a change in the shape of the electron yield curve.

Herein, we report the first observation of concentration-dependent electronic properties of Na–ammonia nanoclusters with sizes in the low nanometer range, covering the whole range from nonmetallic to metallic behavior. The clusters allow us to confine a varying amount of metal to a varying number of solvent molecules. The study of such entities of various compositions and sizes allows for the quantification of the smallest entity size and composition that exhibits a phase transition that closely resembles the TMS in bulk solutions, which should help further the understanding of the microscopic properties of the bulk solutions.

We use a previously described velocity map photoelectron imaging (VMI) spectrometer[11] to gain information on the eBE and the photoelectron angular distribution (β-parameter) of $Na_m(NH_3)_n$ clusters with sizes in the low nanometer range and average MPMs between 1.2 and 8.8. The average and maximum cluster diameters are approximately 2.4 nm and 3.6 nm, corresponding to 200 and 650 NH_3 molecules, respectively. Mass spectra are shown and discussed in the Supporting Information in Section S1.1, while Section S1.2 describes the determination of the average MPM (Supporting Information, Figure S2). The concentration-dependent photoelectron spectra are presented in Figure 1. Representative photoelectron images are provided in the Supporting Information, Section S2, Figure S4. The Supporting Information Section S1.3 describes the calculation of the cluster temperatures for the measurements in Figure 1 (see the Supporting Information, Table S1). The two spectra with the lowest MPM (≤ 1.3) in Figure 1 are dominated by singly Na-doped clusters ($Na(NH_3)_n$), while the contribution of singly-doped clusters to the PES for higher MPMs is negligible. The spectra between MPMs of 1.9 and 6.2 consist of a low and a high energy band, which are referred to as B_{solv} and B_{surf}, respectively. The relative intensity of B_{surf} versus B_{solv} increases strongly with

[*] M. Sc. S. Hartweg, Dr. A. H. C. West, Dr. B. L. Yoder, Prof. Dr. R. Signorell
Laboratory of Physical Chemistry, Department of Chemistry and Applied Biosciences, ETH Zürich
Vladimir-Prelog-Weg 2, 8093 Zürich (Switzerland)
E-mail: rsignorell@ethz.ch

Supporting information for this article can be found under: http://dx.doi.org/10.1002/anie.201604282.

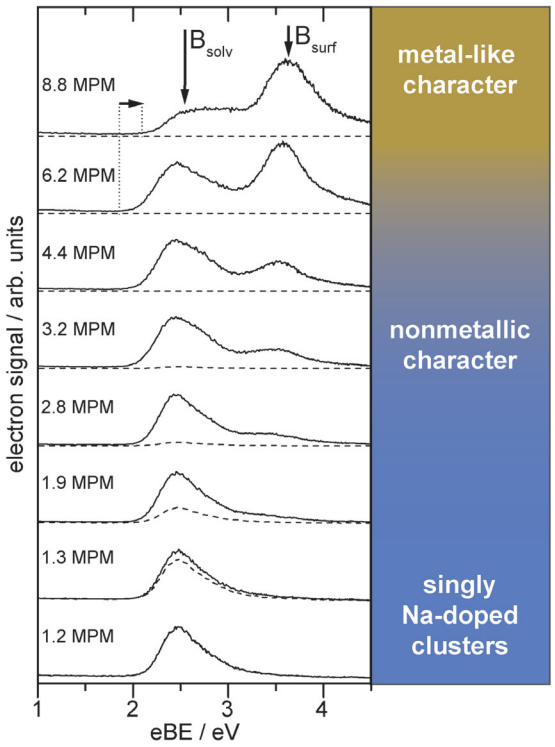

Figure 1. Photoelectron spectra of $Na_m(NH_3)_n$ clusters as a function of the MPM. B_{solv} and B_{surf} indicate structures with internally solvated Na atoms and surface-bound Na atoms, respectively. The dashed lines indicate the contribution of singly Na-doped clusters to the PES. The horizontal arrow indicates the shift of the PET_{solv} at 8.8 MPM. The colors indicate the colors of the corresponding bulk phases.

increasing MPM, and the eBE at the maximum of B_{surf} (eBE_{surf}) slightly shifts to higher energies (Table 1). The threshold (PET_{solv}) and the binding energy (eBE_{solv}) at the maximum of B_{solv} are insensitive to the MPM value up to 6.2 MPM. At 8.8 MPM, the position and shape of B_{solv} changes suddenly and pronouncedly. PET_{solv} shifts to a higher value and the band broadens with a plateau extending from eBE_{solv} values of approximately 2.3 to 3 eV. This sudden change in the band appearance indicates a drastic change in the electronic properties of the sodium–ammonia clusters.

Table 1: Photoelectric threshold values (PET_{solv}) and electron binding energies (eBE_{solv}; eBE_{surf}) for the two bands B_{solv} and B_{surf} observed in the PES in Figure 1. The β-parameters of the two bands are $\beta_{solv} = 0.14 \pm 0.10$ and $\beta_{surf} = 0.38 \pm 0.10$, respectively.

MPM[a]	PET_{solv}	eBE_{solv}	eBE_{surf}
0.11–0.83[a]	1.45–1.42	–	–
1.2; singly Na-doped[b]	2.0	2.5	–
1.3; singly Na-doped[b]	2.0	2.5	–
1.9[b]	1.9	2.5	3.4
2.8[b]	1.9	2.5	3.5
3.2[b]	1.9	2.5	3.5
4.4[b]	1.9	2.5	3.5
6.2[b]	1.9	2.5	3.6
8.8[b]	2.1	2.3–3.0	3.6
10.0–16.2[a]	1.50–1.60	–	–

[a] Ref.[10b]; bulk solutions. [b] This work; nanodroplets.

The finite size of the clusters leads to specific cluster effects in the PES in addition to bulk-like features. We distinguish surface and confinement contributions to these finite-size effects. Based on the present measurements (Figure 1 and Table 1), the ab initio calculations for small $Na_2(NH_3)_n$ clusters in Figure 2 (Supporting Information, Section S3), previous size-dependent photoelectron studies on singly-doped $Na(NH_3)_n$ clusters,[11b,12] and the bulk electron yield measurements,[10] we assign B_{solv} to internally solvated Na atoms and B_{surf} to surface-bound Na atoms. First, the ab initio results in Figure 2 reproduce the experimentally observed order and difference (ca. 1 eV) between B_{solv} and B_{surf} for $n \gtrsim 20$, at which point they level off. Additionally, the calculations reveal that surface-bound Na structures only appear when more than one Na is present, consistent with the experimental observation.

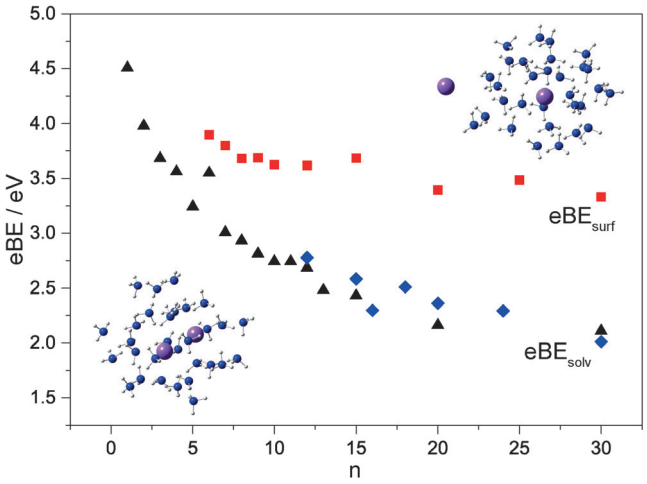

Figure 2. Calculated electron binding energies for $Na_2(NH_3)_n$ clusters as a function of cluster size n. eBE_{surf} corresponds to structures with surface-bound Na atoms (red squares) and eBE_{solv} to structures with internally solvated Na atoms (black triangles and blue diamonds). The triangles and diamonds represent structures with shorter and longer Na–Na distances, respectively. See also the Supporting Information, Section S3.

Second, we have shown in Ref. [11b] that the approximate position of the eBE is mainly determined by the solvation of the Na ion and less by the location of the electron (surface vs. bulk). (Note the fundamental difference to anionic clusters, which have an excess electron but no counter-ion.[3a,13]) The surface-bound Na atoms in the $Na_m(NH_3)_n$ clusters are only partially solvated, similar to the situation in small singly-doped $Na(NH_3)_n$ with $n \leq 3$. Therefore, it is not surprising that both have similar eBEs (ca. 3.5 eV and 3.2–3.4 eV,[11b] respectively). Fully solvated singly-doped $Na(NH_3)_n$ clusters ($n \gtrsim 6$), in contrast, have eBEs below approximately 2.7 eV; that is, close to the eBE_{solv} values for internally solvated Na atoms in multiply-doped nanoclusters. This dependence of the eBE on the degree of solvation of the Na ion (partially vs. fully solvated) clearly supports the assignment of B_{solv} and B_{surf} to

internally solvated and surface-bound Na atoms, respectively. Third, this assignment is reinforced by the fact that the PET_{solv} values of the clusters are close to the bulk PET_{solv} values (Table 1), considering that the confinement effects in nanoclusters lead to a shift of the threshold values to slightly higher energies compared with the bulk values. Typical shifts between clusters of this size and the bulk are approximately 0.5 eV (see reported data for singly-doped and anionic clusters[11b,13a,b,14]). The values of eBE_{surf} for the nanoclusters, in contrast, are too far from bulk PET_{solv} values to justify an assignment of B_{surf} to any bulk-like structures. Last, the smaller value of the anisotropy parameter, $\beta_{solv} = 0.14 \pm 0.10$, for B_{solv} compared with $\beta_{surf} = 0.38 \pm 0.10$ for B_{surf} is also consistent with the general expectation for surface and solvated structures. The photoelectron of an internally solvated Na atom is expected to experience more scattering with the cluster compared with the surface-bound Na, and thus to have a lower β-parameter.[11b,12b,15] All these arguments corroborate our assignment of B_{solv} and B_{surf} to internally solvated Na atoms and surface-bound Na atoms, respectively.

The cluster-equivalent to the TMS in bulk sodium–ammonia solutions can only occur for the bulk-like B_{solv} feature, but not for the cluster-specific B_{surf} band. We therefore focus the following discussion on the evolution of B_{solv} with increasing MPM. For singly Na-doped clusters (1.2 and 1.3 MPM), the indicated MPM cannot be compared with the corresponding bulk concentrations because only one Na atom per cluster is present, while in the bulk several Na atoms are present at these MPM values, leading to specific electron–electron, ion–electron, and ion–ion interactions.[2,3d,4] The closest bulk equivalent for the singly Na-doped clusters are dilute solutions ($10^{-3} \lesssim$ MPM $\lesssim 10^{-1}$), in which association between the electrons and ions (ion pairing) takes place. In the cluster, the association is enforced by confinement. Both association and confinement are responsible for the shift between the cluster PET_{solv} and the bulk PET_{solv} for MPMs $\leq$ 1.3 (Table 1). At these low concentrations, the clusters are likely solid, whereas they are rather liquid at higher MPMs (Supporting Information, Table S1 in Section S1.3).

A meaningful comparison between the bulk and cluster concentrations is only possible when several Na atoms are confined within a cluster; that is, above approximately 1.9 MPM. Between 1.9 and 6.2 MPM, B_{solv} shows essentially no spectral changes, and the spectral features are largely identical to those of the singly-doped clusters (Figure 1). This spectral insensitivity provides a strong indication that the cluster ensemble in this MPM range is still dominated by nonmetallic behavior. In bulk solutions, this is the range in which spin-pairing and other association phenomena can occur. However, they are not expected to have a strong influence on the electronic behavior.[3d,4] For temperatures below 231.5 K, this is the concentration range in which liquid–liquid phase separation and other instabilities are found in the bulk.[3d,4]

The following independent observations are fully consistent with an assignment of the spectral change of B_{solv} between 6.2 and 8.8 MPM (Figure 1) to the droplet equivalent of the nonmetal-to-metal transition in the bulk: 1) The transition occurs at approximately 8.8 ± 2.2 MPM (Supporting Information, Figure S2) and is in the same MPM range as the TMS in bulk solutions at similar temperatures.[3d,4–9] The lack of signs for a phase transition at MPMs ≤ 6.2 (Figure 1) could be a cluster specific effect or simply an effect of the cluster temperature, which increases with the MPM (Supporting Information, Table S1). Even though cluster specific effects should not be excluded, the estimated cluster temperatures in Table S1 already provide a potential explanation. For clusters below approximately 8.8 MPM, the cluster temperatures are outside the temperature range in which the TMS in the bulk has been investigated and reported. 2) The phase transition leads to similar changes in the PES as observed in the bulk electron yield spectrum;[10] that is, the value of PET_{solv} is slightly higher (0.2 eV) for the metallic compared with the nonmetallic solution and the shape of the spectrum changes. As before, the difference between the absolute values of the PET_{solv} of the nanoclusters and the bulk at MPMs ≥ 8.8 is likely due to confinement effects similar to those in large singly-doped clusters.[11b,14,16] 3) We do not observe an equivalent spectral change in small $Na_m(NH_3)_n$ clusters with less than a few tens of molecules per cluster (Supporting Information, Section S4). These clusters are too small to exhibit bulk-like behavior and thus to show a phase transition. 4) We do not observe such a phase transition in large Na-doped dimethyl ether nanodroplets over the range of conditions investigated (Supporting Information, Section S5). In contrast to liquid Na-ammonia solutions, liquid Na-dimethyl ether bulk mixtures do not show a TMS, and therefore a TMS should not be observable in Na-doped dimethyl ether clusters.[11b] Consistent with this expectation, the onset and the shape of B_{solv} in the PES of Na-dimethyl ether clusters in the Supporting Information Figure S8 do not change significantly with changing MPM; that is, the characteristic shift and plateau of PET_{solv} observed for Na-ammonia clusters at 8.8 MPM in Figure 1 are only found when a TMS is expected. 5) The characteristic changes of B_{solv} at 8.8 MPM in Figure 1 cannot arise from bare Na_m clusters because their eBEs are higher, typically in the region around and above B_{surf}[17] (Supporting Information, Section 1.1). The spectral changes in the PES at 8.8 MPM in Figure 1 are obviously unique to large Na-ammonia clusters and MPMs in this range. The consistency of all the above observations, in particular the agreement in terms of MPM range and temperature with the TMS in the bulk solutions, hint that the observed change at 8.8 MPM in Figure 1 is indeed the cluster equivalent of the TMS in bulk. All indications point to a transition to a metal-like cluster phase as the most plausible and consistent explanation. A final proof can of course not be provided from the PES alone.

The metallic behavior in bulk solutions is characterized by delocalized electrons with a collective behavior. At the same MPM, the electron and the Na-ion densities are the same in the bulk solutions and in the clusters. This would support a metal-like behavior of the clusters above the phase-transition MPM. However, the influence of the confinement also needs to be taken into account in this context. As a final remark, we also note that the TMS in metal clusters[18] is different from the present phase transition in molecular

clusters, regarding structure, confinement, and number of Na atoms. The structure and thus the electronic properties of even relatively large metal clusters can distinctly vary with cluster size (for example, the existence of magic clusters). This is not the case for the molecular nanosolutions considered here, which have essentially no size-dependent structure, except for the very smallest clusters with only very few solvent molecules. Therefore, the only factor that changes with size is the confinement, which, for an average cluster size of 100–200 solvent molecules as reported here, is less tight than for the typical metal cluster cases. Confinement effects might thus be less important for the TMS in the present molecular nanosolutions.

In conclusion, we demonstrate that cluster solvation studies provide a route to obtain concentration-dependent PES of Na–ammonia solutions, which are not accessible for bulk solutions. The results are consistent with an assignment of the characteristic changes observed in the PES at approximately 8.8 MPM to the cluster analogue of the well-known nonmetal-to-metal transition in Na–ammonia bulk solutions. The work reveals that on average approximately 100–200 ammonia molecules are required for the phase transition to be observed. This is an intriguing result as this size range is within the reach of modern atomistic simulation techniques. Studies on finite-sized systems, such as the present one, pave the way for a molecular-level understanding of the behavior of these remarkable solutions.

Experimental Section

Solvent nanoclusters are formed in a supersonic expansion and doped with Na atoms by traversing a pickup cell containing different amounts of Na vapor.[11a,19] The clusters are then ionized with the fourth harmonic (266 nm) of a Nd:YAG laser. The cluster size distribution is determined by mass spectrometry.[11a,19] The photoelectron images were analyzed following published procedures.[11]

Acknowledgements

We are grateful to the anonymous referees for the helpful comments, and we thank Alexander Malär for his contribution to the Na-dimethyl ether measurements and Daniel Zindel for the synthesis of deuterated dimethyl ether. Funding from the Swiss National Science Foundation (SNSF_200020_159205) and ETH Zurich (ETH-01 15-2) is acknowledged.

Keywords: electron binding energy · electronic structure · metal–ammonia solutions · photoelectron anisotropy · solvated electrons

How to cite: *Angew. Chem. Int. Ed.* **2016**, *55*, 12347–12350
Angew. Chem. **2016**, *128*, 12535–12538

[1] a) P. P. Edwards, *Adv. Inorg. Chem. Radiochem.* **1982**, *25*, 135–185; b) D. Holton, P. Edwards, *Chem. Br.* **1985**, *21*, 1007–1013; c) J. M. Thomas, P. P. Edwards, V. L. Kuznetsov, *ChemPhysChem* **2008**, *9*, 59–66; d) W. Weyl, *Ann. Phys.* **1864**, *121*, 601–612.
[2] E. Zurek, P. P. Edwards, R. Hoffmann, *Angew. Chem. Int. Ed.* **2009**, *48*, 8198–8232; *Angew. Chem.* **2009**, *121*, 8344–8381.
[3] a) J. M. Herbert in *Reviews in Computational Chemistry, Vol. 28* (Eds.: A. L. Parrill, K. B. Lipkowitz), Wiley, Hoboken **2015**, pp. 391–517; b) P. Vöhringer, *Annu. Rev. Phys. Chem.* **2015**, *66*, 97–118; c) J. M. Herbert, L. D. Jacobson, *J. Phys. Chem. A* **2011**, *115*, 14470–14483; d) G. N. Chuev, P. Quémerais, J. Crain, *J. Chem. Phys.* **2007**, *127*, 244501.
[4] G. N. Chuev, P. Quémerais, *J. Chem. Phys.* **2008**, *128*, 144503.
[5] a) A. J. Birch, D. K. C. MacDonald, *Trans. Faraday Soc.* **1948**, *44*, 735–742; b) R. A. Ogg, Jr., *Phys. Rev.* **1946**, *69*, 243–244; c) O. Ruff, J. Zedner, *Ber. Dtsch. Chem. Ges.* **1908**, *41*, 1948–1960.
[6] P. D. Schettler, Jr., A. Patterson, Jr., *J. Phys. Chem.* **1964**, *68*, 2865–2869.
[7] a) C. A. Kraus, *J. Am. Chem. Soc.* **1907**, *29*, 1557–1571; b) C. A. Kraus, W. W. Lucasse, *J. Am. Chem. Soc.* **1922**, *44*, 1949–1953; c) P. Chieux, M. J. Sienko, *J. Chem. Phys.* **1970**, *53*, 566–570.
[8] D. S. Kyser, J. C. Thompson, *J. Chem. Phys.* **1965**, *42*, 3910–3918.
[9] J. C. Wasse, S. Hayama, S. Masmanidis, S. L. Stebbings, N. T. Skipper, *J. Chem. Phys.* **2003**, *118*, 7486–7494.
[10] a) H. Aulich, B. Baron, P. Delahay, R. Lugo, *J. Chem. Phys.* **1973**, *58*, 4439–4443; b) J. Häsing, *Ann. Phys.* **1940**, *37*, 509–533.
[11] a) B. L. Yoder, A. H. C. West, B. Schläppi, E. Chasovskikh, R. Signorell, *J. Chem. Phys.* **2013**, *138*, 044202; b) A. H. C. West, B. L. Yoder, D. Luckhaus, C.-M. Saak, M. Doppelbauer, R. Signorell, *J. Phys. Chem. Lett.* **2015**, *6*, 1487–1492.
[12] a) A. H. C. West, B. L. Yoder, D. Luckhaus, R. Signorell, *J. Phys. Chem. A* **2015**, *119*, 12376–12382; b) R. Signorell, B. L. Yoder, A. H. C. West, J. J. Ferreiro, C.-M. Saak, *Chem. Sci.* **2014**, *5*, 1283–1295.
[13] a) H. W. Sarkas, S. T. Arnold, J. G. Eaton, G. H. Lee, K. H. Bowen, *J. Chem. Phys.* **2002**, *116*, 5731–5737; b) G. H. Lee, S. T. Arnold, J. G. Eaton, H. W. Sarkas, K. H. Bowen, C. Ludewigt, H. Haberland, *Z. Phys. D* **1991**, *20*, 9–12; c) R. M. Young, D. M. Neumark, *Chem. Rev.* **2012**, *112*, 5553–5577.
[14] C. Steinbach, U. Buck, *J. Chem. Phys.* **2005**, *122*, 134301.
[15] A. H. C. West, B. L. Yoder, R. Signorell, *J. Phys. Chem. A* **2013**, *117*, 13326–13335.
[16] C. P. Schulz, A. Gerber, C. Nitsch, I. V. Hertel, *Z. Phys. D* **1991**, *20*, 65–67.
[17] a) A. Herrmann, S. Leutwyler, E. Schumacher, L. Wöste, *Helv. Chim. Acta* **1978**, *61*, 453–487; b) K. Wong, G. Tikhonov, V. V. Kresin, *Phys. Rev. B* **2002**, *66*, 125401; c) C. Steinbach, U. Buck, *Phys. Chem. Chem. Phys.* **2005**, *7*, 986–990; d) M. M. Kappes, M. Schär, U. Röthlisberger, C. Yeretzian, E. Schumacher, *Chem. Phys. Lett.* **1988**, *143*, 251–258.
[18] a) B. von Issendorff, O. Cheshnovsky, *Annu. Rev. Phys. Chem.* **2005**, *56*, 549–580; b) O. C. Thomas, W. Zheng, S. Xu, K. H. Bowen, Jr., *Phys. Rev. Lett.* **2002**, *89*, 213403; c) A. Aguado, A. Vega, A. Lebon, B. von Issendorff, *Angew. Chem. Int. Ed.* **2015**, *54*, 2111–2115; *Angew. Chem.* **2015**, *127*, 2139–2143; d) J. Heinzelmann, P. Kruppa, S. Proch, Y. D. Kim, G. Ganteför, *Chem. Phys. Lett.* **2014**, *603*, 1–6; e) G. L. Gutsev, C. A. Weatherford, B. R. Ramachandran, L. G. Gutsev, W. J. Zheng, O. C. Thomas, K. H. Bowen, *J. Chem. Phys.* **2015**, *143*, 044306.
[19] a) B. Schläppi, J. J. Ferreiro, J. H. Litman, R. Signorell, *Int. J. Mass Spectrom.* **2014**, *372*, 13–21; b) B. L. Yoder, J. H. Litman, P. W. Forysinski, J. L. Corbett, R. Signorell, *J. Phys. Chem. Lett.* **2011**, *2*, 2623–2628.

Received: May 3, 2016
Revised: August 14, 2016
Published online: August 29, 2016

